IEEE Open Journal of
Antennas and Propagation

Received 10 August 2022; revised 1 September 2022; accepted 6 September 2022. Date of publication 15 September 2022;
date of current version 28 September 2022.

Digital Object Identifier 10.1109/OJAP.2022.3206899

A Liquid-Metal-Based Crossed-Slot Antenna With Polarization and Continuous-Frequency Reconfiguration

YI ZHOU (Graduate Student Member, IEEE), GE ZHAO, XIAO YU LI (Graduate Student Member, IEEE), AND MEI SONG TONG

Department of Electronic Science and Technology, Tongji University, Shanghai 201804, China

CORRESPONDING AUTHOR: M. S. TONG (e-mail: mstong@tongji.edu.cn)

This work was supported in part by the National Natural Science Foundation of China under Project 62071331, and in part by the International Science and Technology Collaboration Project of Shanghai Committee of Science and Technology, Shanghai, China, under Project 21500714400.

ABSTRACT Aiming to the limitations of traditional reconfigurable antennas, this paper proposes a novel reconfigurable antenna that can achieve four polarizations and continuously-tunable frequency. The proposed antenna is based on liquid metal, i.e., eutectic gallium and indium (EGaIn). The pattern of the slots can be controlled by changing the amount of the liquid metal inserted in the 3-D printed channels. The antenna can work under four polarization modes: left-hand circular polarization (LHCP), right-hand circular polarization (RHCP), and two orthogonal linear polarization (LP) modes. Under the LP modes, the working frequency of the antenna can be tuned continuously from 1.82 GHz to 2.0 GHz. The measured results agree with the simulated ones, which validate the performance of proposed antenna.

INDEX TERMS Continuous-frequency reconfiguration, polarization reconfiguration, liquid metal, patch antenna.

I. INTRODUCTION

MODERN communication has long been calling for antennas that can be adapted to various situations, which makes reconfigurable antenna one of the most popular research topics at present. Most reconfigurable antennas are based on photoconductive devices, changeable materials like liquid crystal, or electrically controlled components like radio-frequency microelectromechanical systems (RF-MEMS) and PIN-Diodes [1], [2], [3], [4]. However, these components usually have fixed physical structures or limited work modes, which may limit the antennas' reconfigurability. Liquid metal, as a fluid material, can help break the limitation.

Liquid metal has been applied in diverse fields, such as flexible circuits, wearable devices, and soft sensors [5], [6]. Antennas are of no exception [7], [8], [9], [10], [11], [12], [13]. Among all the liquid metal, eutectic gallium and indium (EGaIn) stands out for its relatively high conductivity: $\sigma = 3.4 \times 10^6$ S/m. Its non-toxic feature also indicates its broad application prospect. Most importantly, it can stably remain fluid at room temperature. Therefore, it can provide more possibilities for antenna reconfiguration.

We proposed a polarization and continuous-frequency reconfigurable antenna based on EGaIn. The configuration and the prototype of the antenna are proposed in Fig. 1. By controlling the amount of the liquid metal inserted into the 3-D printed channels attached to the patch, the pattern of the crossed-slots can be reconfigured.

The novelty of the proposed design focuses on its high reconfigurability. By making use of the fluidity of liquid metal, the crossed-slots can be changed into arbitrary patterns. The antenna can thus be reconfigured in both polarization and frequency. It has four polarization modes: LHCP, RHCP, and two orthogonal LP modes. And its working frequency can be tuned continuously, which is hard to achieve by using traditional reconfiguration methods.

This work is an expansion of our previous paper [14]. More measurement results and design details are added, and the theory is further discussed.

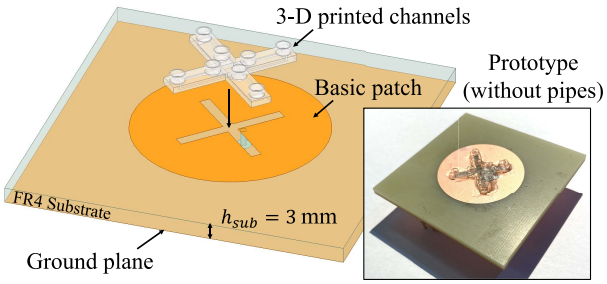

FIGURE 1. The configuration and the prototype of the proposed antenna.

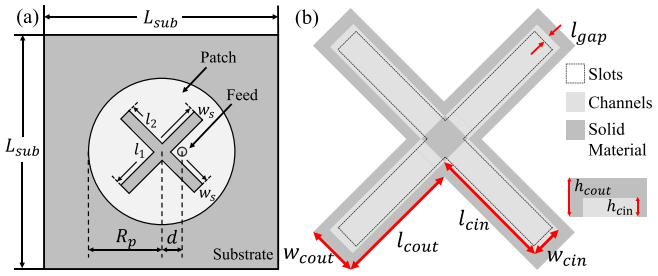

FIGURE 2. The geometry and dimensions of the design (mm): (a) The basic patch: L_{sub} = 65, R_p = 18.5, d = 2.5, w_s = 2, and l_1 = l_2 = 21. (b) The 3-D printed channel: w_{cout} = 4, l_{cout} = 20, w_{cin} = 2.5, l_{cin} = 9.7, h_{cout} = 1.3, h_{cin} = 0.3, and l_{gap} = 0.5.

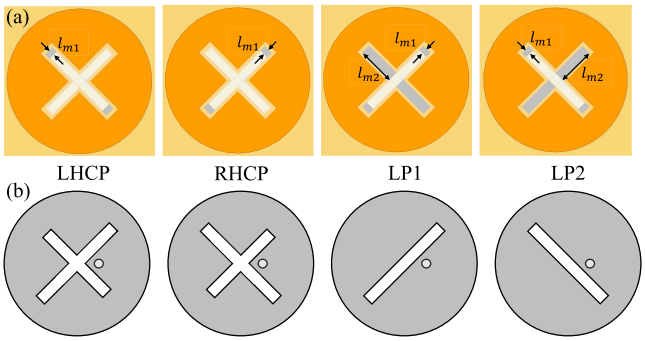

FIGURE 3. The patterns under four polarization states: (a) Patterns with slots covered by liquid metal. (b) Corresponding patterns of uncovered slots.

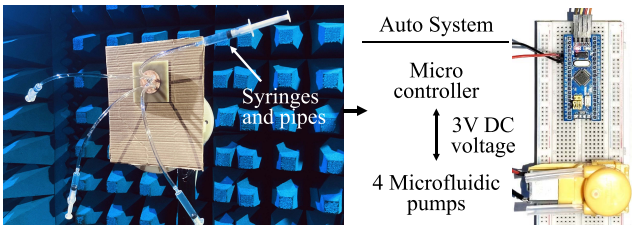

FIGURE 4. The antenna is measured in anechoic chamber. The liquid metal can be controlled by syringes or the automatic controlling system.

II. DESIGN GEOMETRY

A. BASIC PATCH

The basic element of the antenna is a circular patch with crossed-slots in the middle, as shown in Fig. 2(a). Circular patch is chosen because it is more suitable for probe feeding, and it also occupies less area comparing to rectangular structure. The copper patch is based on a 3-mm-thick FR4 substrate ($\varepsilon_r = 4.4$, $tan\delta = 0.02$ at 1.0 GHz).

Crossed-slots has been frequently used in circular-polarized antennas [15], [16], [17]. Reconfigurable antennas also make use of crossed-slots to realize polarization reconfiguration [18], [19], [20], [21].

B. 3-D PRINTED CHANNELS

The channels used to contain liquid metal are 3-D printed with Formlabs Clear SLA resin ($\varepsilon_r = 2.8$, $tan\delta = 0.021$ at 4.0 GHz) [22]. The stereolithography 3-D printing technology ensures the accuracy of the model.

The widths of the channels are slightly larger than the slots, so that the liquid metal can cover the slots properly. The channels are attached to the patch by Ultraviolet (UV) glue ($\varepsilon_r = 3.9$, $tan\delta = 0.03$ at 1.0 MHz). The specific geometry of the channels is illustrated in Fig. 2(b). There are four channels in total.

III. RECONFIGURATION

A. RECONFIGURABLE MODES

Each channel has two openings at the ends as shown in Fig. 1. The liquid metal EGaIn is inserted into the channels through pipes connected to the openings. By controlling the amount of the liquid metal inserted into each channel, four polarization modes can be achieved as shown in Fig. 3(a). The corresponding patterns of the crossed-slots are given in Fig. 3(b).

Under CP modes, two opposite channels are empty, and the lengths of the liquid metal in the other two channels are $l_{m1} = 1.5$ mm.

Under LP modes, two opposite channels are fully filled with liquid metal with lengths of $l_{m2} = 9.7$ mm. The lengths of the liquid metal in the other two channels are denoted as l_{m1}. With l_{m1} changing, the working frequency can be tuned continuously.

In previous works [18], [19], the lengths of the slots are usually controlled by PIN-diodes, in which way the antennas can only be reconfigured discontinuously because of PIN-diode's binary states and fixed position. So, here we propose a new method to reconfigure these slots. By covering the slots with the liquid metal, the lengths of the slots can be changed arbitrarily.

B. CONTROLLING METHODS

While controlling the working mode of the antenna system, syringes can be used to insert or withdraw the liquid metal manually as shown in Fig. 4. Automatic controlling system in Fig. 4 is designed to improve the speed and the accuracy of the process.

The automatic control system consists of a microcontroller, a 3 V DC power supply, and four 2-direction microfluidic pumps. The microcontroller we use is STM32F103C8T6 minimum system board based on ARM cortex. The microfluidic pumps are WX1/ZL Micro

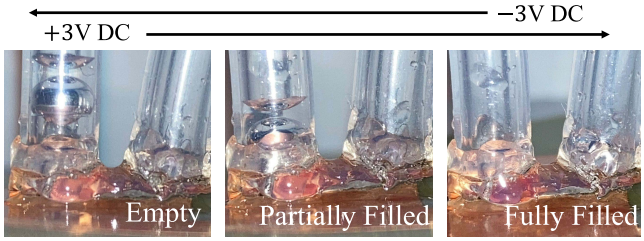

FIGURE 5. The reversible controlling process of liquid metal by microfluidic pumps.

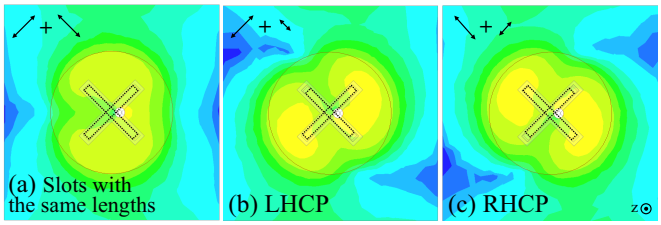

FIGURE 6. Simulated current density on the ground plane from the top view at $\phi = 0$. (a) Antenna with the same slots. (b) LHCP mode. (c) RHCP mode.

Peristaltic from JIHPUMP company with two pumping directions. The pumps can be controlled by applying a DC voltage between 3 and 6 V. The maximum rate of flow is 14 mL/min under 3 V power supply. The rate of flow is small enough to ensure the accuracy in controlling the lengths of the liquid metal.

We use 0.1 mol/L NaOH ($\sigma \approx 0.5$ S/m) solution as carrier liquid. The solution can help remove the oxide coating of EGaIn, and ensure the smooth movement of the liquid metal.

According to the dimensions of the channels listed in the description of Fig. 2, the amount of the liquid metal needed to fill the entire channel is approximately 2.9 mm^3, which can be measured by syringes. The controlling process of the liquid metal is shown in Fig. 5. By applying +3 V DC voltage to the positive pin of the pump, the liquid metal can be inserted into the channel. While applying −3 V, EGaIn is pumped out of the channel back to the pipe. The whole process is reversible, and is controlled by STM32 microcontroller by digital signals through I/O pins.

The time needed to fill an empty channel is 12.4 ms. And the time needed for l_{m1} to grow from 0 to 1.5 mm is 1.8 ms.

STM32F103C8T6 minimum system board with 16 MHz clock speed can ensure the precision of the control. The minimum change in the length of the liquid metal can reach 3.8×10^{-5} mm, which takes two clock cycles. The errors can be eliminated by manually calibrating the initial state of the system.

IV. DESIGN ANALYSIS

A. FORMATION OF POLARIZATION

Circular polarization can be equivalent to a combination of two orthogonal linearly-polarized components. Here, we let $\mathscr{E}_1$ and $\mathscr{E}_2$ represent two linearly polarized waves that are perpendicular to each other. Their magnitudes are $|\mathscr{E}_1| = E_1$ and $|\mathscr{E}_2| = E_2$, respectively. For strictly circular-polarized waves (AR = 0 dB), these components should meet the conditions that

$$E_1 = E_2, \tag{1}$$

$$\phi_1 - \phi_2 = \pm\left(2n + \frac{1}{2}\right)\pi, \quad n = 0, 1, 2, \ldots, \tag{2}$$

where ϕ_1 and ϕ_2 are the phases of the two waves.

Above equations show that, for a circular-polarized wave, the magnitudes of the two components should be equal, and their phases should have a difference of odd multiples of $\pi/2$. In practical applications, we define the waves with AR < 3 dB as circular-polarized, so the above two conditions do not need to be strictly satisfied.

For the proposed antenna, we achieve circular polarization through the structure of crossed-slots. The radiated wave can be considered as the superposition of the wave radiated by each of the two slots.

From condition (2), the slots should be perpendicular to each other in order to generate two orthogonal waves. To satisfy condition (1), we have to make the lengths of the two slots similar. However, when the slots are of the same lengths, the radiated wave is not circular-polarized as can be seen from the current density distribution on the ground plane from Fig. 6(a).

By making one of the slots slightly shorter than the other, the current density grows larger and tends to rotate as shown in Fig. 6(b) and (c). The radiation can be regarded as the mapping of the current density distribution in the far field. So, circular-polarized wave is thus generated.

Whether the radiated wave is LHCP or RHCP is determined by which of the two slots is shorter. In other words, it depends on which wave component leads the other. The difference can be corresponded to the symbol "±" in (2).

B. PATCH MODEL AND SIZE

By applying the cavity model, the size of the circular patch under TM_{mn0} mode can be approximately calculated by

$$a = \frac{a_e}{\left\{1 + \frac{2h}{\pi\varepsilon_r a_e}\left[ln\left(\frac{\pi a_e}{2h} + 1.7726\right)\right]\right\}^{1/2}}, \tag{3}$$

where h represents the height of the substrate, ε_r is the relative permittivity of the substrate material, and a_e is the effective radius of the patch due to the fringing effect, which can be achieved from

$$a_e = \frac{\chi'_{mn} v_0}{2\pi (f_{re})_{mn0}\sqrt{\varepsilon_r}}, \tag{4}$$

where χ'_{mn} is the zeroes of the derivative of the Bessel function $J_m(x)$, v_0 represents the speed of light in free-space, and $(f_{re})_{mn0}$ is the intended working frequency, respectively.

Proposed antenna works under TM_{110} mode due to the slot structure, so the value of χ'_{mn} should be $\chi'_{11} = 1.8412$.

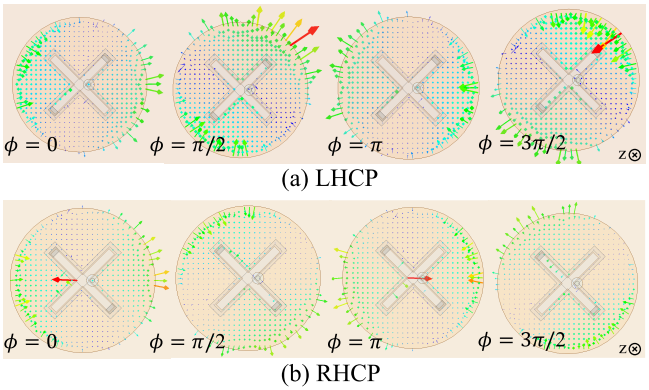

FIGURE 7. Simulated E-field vector for two CP modes from the bottom view: (a) LHCP mode. (b) RHCP mode.

V. SIMULATED AND MEASURED RESULTS

Ansys HFSS is used to simulate the antenna. During the simulation, the liquid metal inserted in each channel is modeled as cube with height of $h_{in} = 0.3$ mm.

Since the two CP modes and the two LP modes are highly symmetrical, we only present the results from one of the same polarization modes.

A. CIRCULAR POLARIZATION

Fig. 7 presents the change in the simulated E-field vector from the bottom view with the phase of the input signal changing. In Fig. 7(a), the E-field vector rotates counterclockwise, which means that the generated wave is left-hand polarized. Similarly, the vector in Fig. 7(b) rotates clockwise, which means that the polarization is right-handed.

Simulated and measured results of S_{11} parameter and axial ratio (AR) are plotted in Fig. 8. It can be seen from Fig. 8(a) that the simulated frequency band of the antenna is 1.89 GHz - 1.98 GHz, and the measured working frequency is 1.85 GHz - 1.92 GHz. The slight shift in the frequency may be caused by the variation in the properties of the FR4 substrate at different frequencies.

In Fig. 8(b), despite the shift in the resonant frequency, both the simulation and the measurement results show that the antenna is well circular-polarized within the working frequency band.

The simulated and measured radiation patterns on XoZ-plane and YoZ-plane under the RHCP mode are plotted in Fig. 9. Co-polarization and cross-polarization radiation patterns are presented in solid line and dash line, respectively. Only RHCP results are presented, since the radiation pattern for LHCP mode is highly symmetrical. The maximum gain of the antenna is 3.5 dBi toward +z direction. The difference between the co-polarization gain and the cross-polarization gain in +z direction is approximately 15 dB, which means that RHCP and LHCP are isolated.

Fig. 10 shows the S_{11} parameter and the AR with different l_{m1} values. It indicates the antenna's sensitivity to the length of l_{m1} under CP modes. The proposed antenna can remain circular-polarized within the working frequency band when

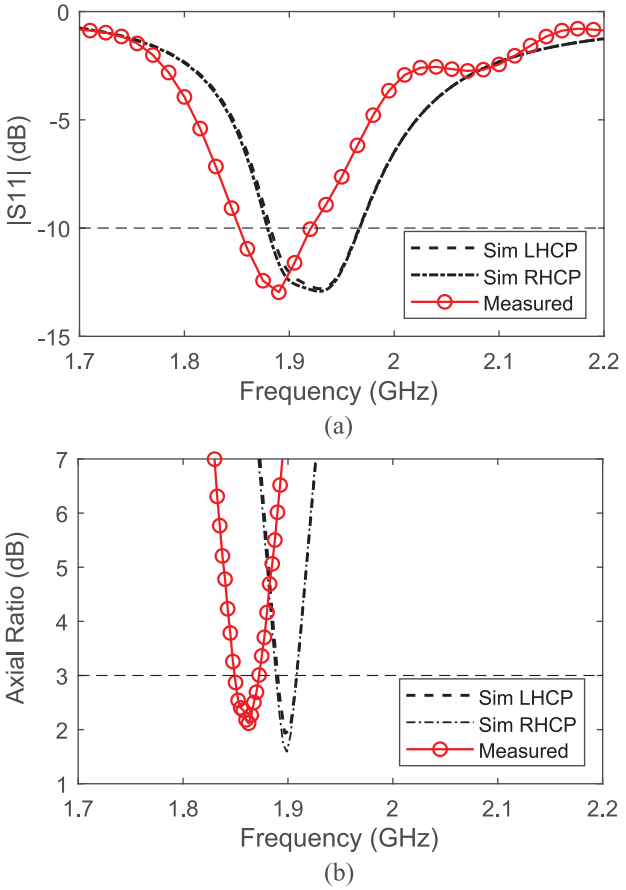

FIGURE 8. Simulated and measured results for LHCP and RHCP modes: (a) S_{11} parameter. (b) Axial ratio.

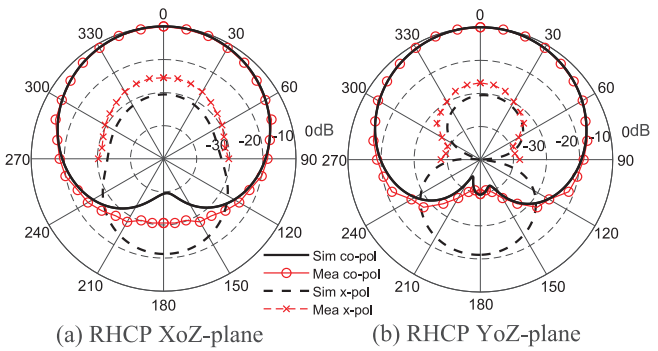

FIGURE 9. Simulated and measured radiation patterns for RHCP modes: (a) XoZ-plane (b) YoZ-plane.

l_{m1} varies from 1.5 to 2.5 mm. So, minor error in the length of l_{m1} will not have a huge influence on the antenna's circular polarization.

B. LINEAR POLARIZATION

Under LP modes, the working frequency of the proposed antenna can be adjusted by the length of l_{m1}. Simulated S_{11} parameters are presented in Fig. 11. With l_{m1} increasing, the working frequency of the antenna will become higher.

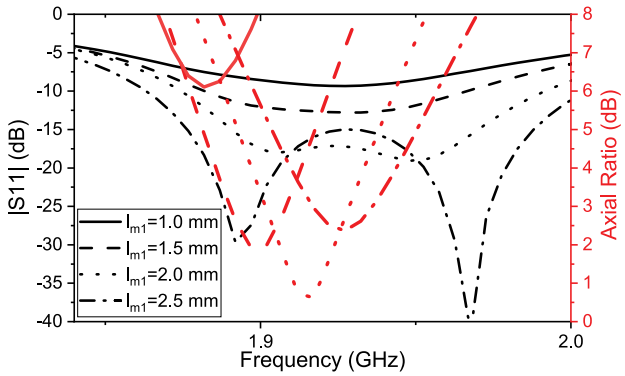

FIGURE 10. The sensitivity of the antenna to the change in l_{m1} under CP modes.

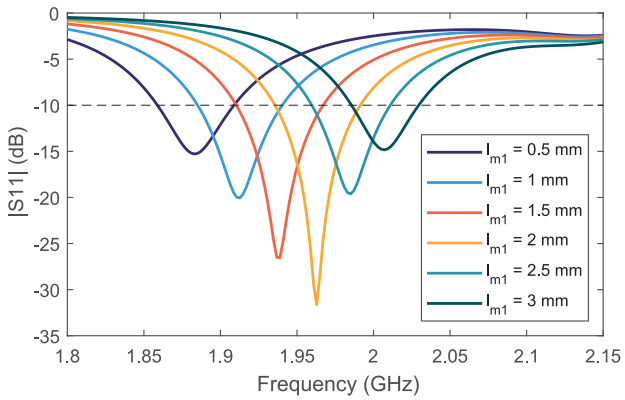

FIGURE 11. Simulated S_{11} parameters for LP modes.

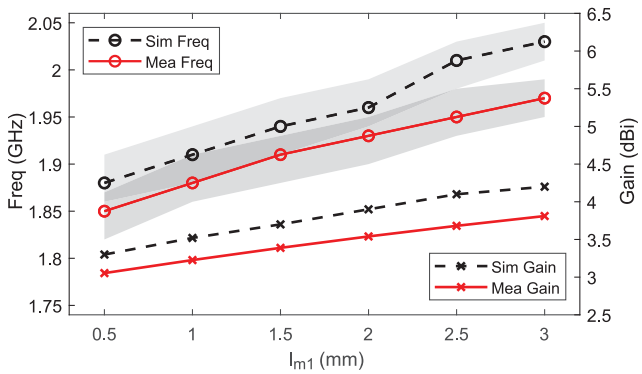

FIGURE 12. Simulated and measured working frequency and gain for LP modes according to the variation in the length of l_{m1}. The gray strips represent the frequency bands.

Fig. 12 demonstrates both working frequency and gain of the antenna under LP mode with different l_{m1}. The comparison between the simulated and measured results are given. Gray areas in Fig. 12 represent the working frequency band. The linear relationship between the working frequency and l_{m1} indicates the feasibility of continuous frequency reconfiguration. The tunable frequency band is from 1.82 GHz to 2.0 GHz according to the measurement.

The measured maximum gain in +z direction can grow from 3.1 dBi to 3.8 dBi with the length of l_{m1} increasing.

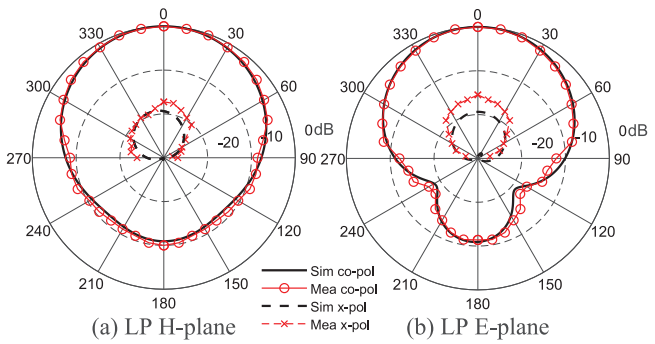

FIGURE 13. Simulated and measured radiation patterns for two LP modes with l_{m1} = 1.5 mm at 1.89 GHz: (a) H-plane. (b) E-plane.

TABLE 1. Comparisons to previous works.

Ref	Mechanism	Reconfigured Properties	Polarization Modes	Frequency Continuity
[10]	LM	Freq	/	Yes
[11]	LM	Pol	LHCP LP	/
[19]	PIN-diode	Pol + Freq	LHCP RHCP LP	No
[23]	LM	Pol + Freq	LHCP RHCP LP	No
Ours	LM	Pol + Freq	LHCP RHCP LP	Yes

For LP modes, the simulated and measured co-polarization and cross-polarization radiation patterns of E-plane and H-plane while $l_{m1} = 1.5$ mm are given in Fig. 13. The cross-polarization gain is much smaller than the co-polarization one, which shows that the antenna is well linear-polarized.

It can be seen from Fig. 12 that a certain frequency point can be achieved by a range of l_{m1}. This increases the allowable range of the controlling error.

VI. COMPARISON

Table 1 lists some comparisons between the proposed antenna and existed works with similar features or structures.

Two reconfigurable antennas based on liquid metal were proposed by Song *et al.* in [10], [11]. These works could only be reconfigurable in one property. Our work can be reconfigured in both polarization and frequency with the similar mechanism, which further improves the reconfigurability of liquid-metal-based antenna.

In [19], Ge *et al.* realized the reconfiguration in both polarization and frequency with the similar geometry of crossed-slots based on PIN-diodes. However, since the positions of PIN-diodes are fixed, the lengths of the slots only have limited states, and the frequency reconfiguration was not continuous. Liu *et al.* made use of the fluid property of EGaIn to design a polarization and frequency reconfigurable antenna in [23]. However, the frequency reconfiguration was also discontinuous. In this work, by inserting liquid metal into 3-D printed channels to cover the crossed-slots, we realize continuous tuning of the slot lengths. Continuous reconfiguration of the frequency is thus be obtained.

VII. CONCLUSION

This paper proposes a polarization and continuous-frequency reconfigurable antenna based on liquid metal. The lengths of the crossed-slots can be changed continuously by controlling the amount of the liquid metal inserted into the 3-D printed channels. Automatic controlling system is introduced to improve the reconfiguration speed and accuracy.

Simulated and measured results are in good agreement. The polarization can switch between LHCP, RHCP, and two orthogonal LP modes. The working frequency under CP modes are from 1.85 GHz to 1.92 GHz. And the frequency under LP modes can be tuned continuously from 1.82 GHz to 2.0 GHz. The radiation is toward the +z direction. The maximum gain under CP modes is 3.5 dBi. And the maximum gain under LP mode ranges from 3.5 dBi to 3.8 dBi.

The proposed antenna has great reconfigurability. The crossed-slots can be changed into arbitrary patterns thanks to the fluidity of the liquid metal. The antenna can thus have four different polarization modes. And since the length of the liquid metal can be changed continuously, tunable working frequency is realized. Liquid metal has improved the reconfigurability of the antenna to a new level, and has broken the limitation of traditional reconfiguration methods.

REFERENCES

[1] C. G. Christodoulou, Y. Tawk, S. A. Lane, and S. R. Erwin, "Reconfigurable antennas for wireless and space applications," *Proc. IEEE*, vol. 100, no. 7, pp. 2250–2261, Jul. 2012.

[2] P. Qin, Y. J. Guo, A. R. Weily, and C. Liang, "A pattern reconfigurable U-slot antenna and its applications in MIMO systems," *IEEE Trans. Antennas Propag.*, vol. 60, no. 2, pp. 516–528, Feb. 2012.

[3] N. Nguyen-Trong, L. Hall, and C. Fumeaux, "A frequency- and polarization-reconfigurable stub-loaded microstrip patch antenna," *IEEE Trans. Antennas Propag.*, vol. 63, no. 11, pp. 5235–5240, Nov. 2015.

[4] J. M. Kovitz, H. Rajagopalan, and Y. Rahmat-Samii, "Design and implementation of broadband MEMS RHCP/LHCP reconfigurable arrays using rotated E-shaped patch elements," *IEEE Trans. Antennas Propag.*, vol. 63, no. 6, pp. 2497–2507, Jun. 2015.

[5] J. Chossat, Y. Park, R. J. Wood, and V. Duchaine, "A soft strain sensor based on ionic and metal liquids," *IEEE Sens. J.*, vol. 13, no. 9, pp. 3405–3414, Sep. 2013.

[6] S. Cheng, Z. Wu, P. Hallbjorner, K. Hjort, and A. Rydberg, "Foldable and stretchable liquid metal planar inverted cone antenna," *IEEE Trans. Antennas Propag.*, vol. 57, no. 12, pp. 3765–3771, Dec. 2009.

[7] G. J. Hayes, J. So, A. Qusba, M. D. Dickey, and G. Lazzi, "Flexible liquid metal alloy (EGaIn) microstrip patch antenna," *IEEE Trans. Antennas Propag.*, vol. 60, no. 5, pp. 2151–2156, May 2012.

[8] D. Rodrigo, L. Jofre, and B. A. Cetiner, "Circular beam-steering reconfigurable antenna with liquid metal parasitics," *IEEE Trans. Antennas Propag.*, vol. 60, no. 4, pp. 1796–1802, Apr. 2012.

[9] G. B. Zhang, R. C. Gough, M. R. Moorefield, K. J. Cho, A. T. Ohta, and W. A. Shiroma, "A liquid-metal polarization-pattern-reconfigurable dipole antenna," *IEEE Antennas Wireless Propag. Lett.*, vol. 17, no. 1, pp. 50–53, Jan. 2018.

[10] L. Song, W. Gao, C. O. Chui, and Y. Rahmat-Samii, "Wideband frequency reconfigurable patch antenna with switchable slots based on liquid metal and 3-D printed microfluidics," *IEEE Trans. Antennas Propag.*, vol. 67, no. 5, pp. 2886–2895, May 2019.

[11] L. Song, W. Gao, and Y. Rahmat-Samii, "3-D printed microfluidics channelizing liquid metal for multipolarization reconfigurable extended E-shaped patch antenna," *IEEE Trans. Antennas Propag.*, vol. 68, no. 10, pp. 6867–6878, Oct. 2020.

[12] C. Wang, Y. Guo, J. C. Yeo, and C. T. Lim, "Improving the radiation efficiency of liquid metal antenna with polarization agility," in *Proc. IEEE Int. Symp. Antennas Propag. USNC/URSI Nat. Radio Sci. Meeting*, Boston, MA, USA, Jul. 2018, pp. 941–942.

[13] F. Xie, J. J. Adams, and M. S. Tong, "An UHF reconfigurable liquid-metal monopole antenna based on a two-dimensional surface," *IEEE Trans. Compon. Packag. Manuf. Technol.*, vol. 11, no. 11, pp. 1980–1987, Nov. 2021.

[14] Y. Zhou and M. S. Tong, "A novel liquid-metal antenna with polarization and continuous-frequency reconfigurability," in *Proc. IEEE Int. Symp. Antennas Propagat. USNC-URSI Radio Sci. Meeting*, Singapore, Dec. 2021, pp. 555–556.

[15] H. Iwasaki, "A circularly polarized small-size microstrip antenna with a cross slot," *IEEE Trans. Antennas Propag.*, vol. 44, no. 10, pp. 1399–1401, Oct. 1996.

[16] C.-Y. Huang, J.-Y. Wu, and K.-L. Wong, "Cross-slot-coupled microstrip antenna and dielectric resonator antenna for circular polarization," *IEEE Trans. Antennas Propag.*, vol. 47, no. 4, pp. 605–609, Apr. 1999.

[17] G. Q. Luo, Z. F. Hu, Y. Liang, L. Y. Yu, and L. L. Sun, "Development of low profile cavity backed crossed slot antennas for planar integration," *IEEE Trans. Antennas Propag.*, vol. 57, no. 10, pp. 2972–2979, Oct. 2009.

[18] M. N. Osman, M. K. A. Rahim, M. F. M. Yussof, M. R. Hamid, and H. A. Majid, "Polarization reconfigurable cross-slots circular patch antenna," in *Proc. Int. Symp. Antennas Propag.*, Nanjing, China, Jan. 2013, pp. 1252–1255.

[19] L. Ge, Y. Li, J. Wang, and C.-Y.-D. Sim, "A low-profile reconfigurable cavity-backed slot antenna with frequency, polarization, and radiation pattern agility," *IEEE Trans. Antennas Propag.*, vol. 65, no. 5, pp. 2182–2189, May 2017.

[20] M. Boti, L. Dussopt, and J.-M. Laheurte, "Circularly polarised antenna with switchable polarisation sense," *Electron. Lett.*, vol. 36, no. 18, pp. 1518–1519, Aug. 2000.

[21] L.-R. Tan, R.-X. Wu, and Y. Poo, "Magnetically reconfigurable SIW antenna with tunable frequencies and polarizations," *IEEE Trans. Antennas Propag.*, vol. 63, no. 6, pp. 2772–2776, Jun. 2015.

[22] V. T. Bharambe, J. Ma, M. D. Dickey, and J. J. Adams, "Planar, multifunctional 3D printed antennas using liquid metal parasitics," *IEEE Access*, vol. 7, pp. 134245–134255, 2019.

[23] Y. Liu, Q. Wang, Y. Jia, and P. Zhu, "A frequency- and polarization-reconfigurable slot antenna using liquid metal," *IEEE Trans. Antennas Propag.*, vol. 68, no. 11, pp. 7630–7635, Nov. 2020.

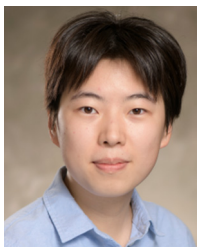

YI ZHOU (Graduate Student Member, IEEE) received the B.Eng. degree in electronic science and technology from Tongji University, Shanghai, China, in 2021. She is currently pursuing the Ph.D. degree in electrical engineering with the University of Illinois at Urbana–Champaign, Urbana, IL, USA. Her current research interests include signal integrity, circuit simulation algorithms, high-frequency circuits, and electromagnetics.

GE ZHAO received the B.S. degree from the Department of Electronic Engineering from East China Normal University, Shanghai, China, in 2019, and the M.S. degree from the Department of Electronic Science and Technology, Tongji University, Shanghai, in 2022.

Her research interest is antenna design, especially metasurface antennas and circularly polarized antennas.

XIAO YU LI (Graduate Student Member, IEEE) received the B.S. degree in communication and information engineering and the M.S. degree in electronic and information engineering from the University of Electronic Science and Technology of China, Chengdu, China, in 2017 and 2020, respectively. He is currently pursuing the Ph.D. degree in Control Science and Engineering with Tongji University, Shanghai, China. His current research interests include reconfigurable antennas and computational electromagnetics.

MEI SONG TONG received the B.S. and M.S. degrees in electrical engineering from the Huazhong University of Science and Technology, Wuhan, China, and the Ph.D. degree in electrical engineering from Arizona State University, Tempe, AZ, USA.

He is currently a Distinguished and Permanent Professor, the Head of Department of Electronic Science and Technology, and the Vice Dean of College of Microelectronics, Tongji University, Shanghai, China. He has also held an adjunct professorship with the University of Illinois at Urbana–Champaign, Urbana, IL, USA, and an honorary professorship with the University of Hong Kong, China. He has published more than 500 papers in refereed journals and conference proceedings and coauthored six books or book chapters. His research interests include electromagnetic field theory, antenna theory and design, simulation and design of RF/microwave circuits and devices, interconnect and packaging analysis, inverse electromagnetic scattering for imaging, and computational electromagnetics. He was a recipient of a Visiting Professorship Award from Kyoto University, Japan, in 2012, and from University of Hong Kong, China, 2013, the Travel Fellowship Award of USNC/URSI for the 31st General Assembly and Scientific Symposium in 2014, the Advance Award of Science and Technology of Shanghai Municipal Government in 2015, the Fellowship Award of JSPS in 2016, the Innovation Award of Universities' Achievements of Ministry of Education of China in 2017, the Innovation Achievement Award of Industry-Academia-Research Collaboration of China in 2019, and the "Jinqiao" Award of Technology Market Association of China in 2020. He advised and coauthored six papers that received the Best Student Paper Award from different international conferences. In 2018, he was selected as the Distinguished Lecturer of IEEE Antennas and Propagation Society from 2019 to 2022. He has served as an Associate Editor or a Guest Editor for several well-known international journals, including *IEEE Antennas and Propagation Magazine*, IEEE TRANSACTIONS ON ANTENNAS AND PROPAGATION, IEEE TRANSACTIONS ON COMPONENTS, PACKAGING AND MANUFACTURING TECHNOLOGY, *International Journal of Numerical Modeling: Electronic Networks, Devices and Fields*, *Progress in Electromagnetics Research*, and *Journal of Electromagnetic Waves and Applications*. He also frequently served as the session organizer/chair, the technical program committee member/chair, and the general chair for some prestigious international conferences. He is a Fellow of the Electromagnetics Academy and Japan Society for the Promotion of Science, and a Full Member (Commission B) of the USNC/URSI. He has been the Chair of Shanghai Chapter since 2014 and the SIGHT Committee in 2018, respectively, in IEEE Antennas and Propagation Society.